A

Project report on

TAYLOR BUBBLE FLOW IN MICROCHANNEL HAVING AN OBSTACLE

By

T SUDHAKAR

ROLL NO: 212ME3322

Under the guidance of

Dr. MANOJ KUMAR MOHARANA

Department of Mechanical Engineering
National Institute of Technology Rourkela
Rourkela 769008 (Odisha)

June 2014

National Institute of Technology Rourkela

CERTIFICATE

This is to certify that the thesis entitled, "TAYLOR BUBBLE FLOW IN MICROCHANNEL HAVING AN OBSTACLE" submitted by Mr. T Sudhakar in partial fulfilment of the requirements for the award of Master of Technology Degree in Mechanical Engineering with specialization in Thermal Engineering at the National Institute of Technology Rourkela is an authentic work carried out by him under my supervision and guidance.

To the best of my knowledge, the matter embodied in the thesis has not been submitted to any other university/institute for the award of any degree or diploma.

Dr. Manoj Kumar Moharana
Department of Mechanical Engineering
National Institute of Technology Rourkela
Rourkela– 769008

Date:

SELF DECLARATION

I, Mr T Sudhakar, Roll No. 212ME3322, student of M. Tech (2012-14), Thermal Engineering at Department of Mechanical Engineering, National Institute of Technology Rourkela do hereby declare that I have not adopted any kind of unfair means and carried out the research work reported in this thesis work ethically to the best of my knowledge. If adoption of any kind of unfair means is found in this thesis work at a later stage, then appropriate action can be taken against me including withdrawal of this thesis work.

T. Sudhakar

T Sudhakar

NIT Rourkela

02 June 2014

ACKNOWLEDGEMENT

I would like to thank and express my gratitude towards my supervisor **Dr. Manoj K Moharana** for his extensive support throughout this project work. I am greatly indebted to him for giving me the opportunity to work with him and for his belief in me during the hard time in the course of this work. His valuable suggestions and constant encouragement helped me to complete the project work successfully. Working under him has indeed been a great experience and inspiration for me.

I would also like to thank Mechanical Engineering Department for providing the CFD lab where I completed the maximum part of my project work.

Place: Rourkela
Date: 2/6/14

T. Sudhakar

T. Sudhakar

ABSTRACT

Taylor bubble flow is one of the important patterns of gas-liquid flow in microchannels. A two-dimensional numerical analysis of the Taylor bubble flow in a microchannel having an obstacle is carried out. The diameter of the microchannel is 0.2 mm. A square shaped obstacle, of size 0.02 × 0.02 mm^2 (i.e., $1/10^{th}$ of the diameter of the microchannel), is placed inside the microchannel. Taylor bubble flow is created using T-junction microchannel. The fluids used for the generation of Taylor bubbles are water and air. As the water and air flows from the two inlets, Taylor bubble is formed at the T-junction. The obstacle is placed at an appropriate distance from the T-junction, where the water and gas fluids are getting mixed, along the downstream such that the stabilized Taylor bubble will touch the obstacle. This shows that the obstacle will be touched by the Taylor bubble which is already in steady motion. The obstacle position is varied along the perpendicular to the direction of fluid flow. Initially the obstacle is kept at the center of the microchannel i.e., it provides an equal space of 0.9 mm on either of its sides inside the microchannel. As the Taylor bubble touches the obstacle it splits into two parts and moves through both sides of the obstacle with a perfect symmetric flow. The bubble joins again and gets to its original form as it passes through the obstacle. Then the obstacle is moved 0.02 mm away from the center towards one side, i.e., it provides a gap of 0.11 mm and 0.07mm on either side of the obstacle respectively. In this case as the Taylor bubble touches the obstacle it doesn't split into two parts rather the whole bubble tries to move to the upper side of the obstacle i.e. maximum area side. Similar phenomenon is observed as the obstacle moves further away from the center line towards one side. The liquid-gas interface is continuously changing its shape due to the disturbance caused by the presence of the obstacle. This creates turbulence inside the liquid plugs present in between the two consecutive bubbles, which is shown by using the velocity vector fields. This may raise hope to enhance more heat and mass transfer in the microchannels by placing multiple obstacles inside the microchannels.

Keywords: Taylor bubble flow, microchannel, T-joint, obstacle, two-phase flow.

Contents

List of Figures

Nomenclature

C Courant number, (-)

Ca Capillary number, (-)

$\vec{F}$ Surface tension force of the fluid, N/m^2

p Pressure force, N/m^2

R Channel radius, m

t Time, sec

q" Heat flux, W/ m^2

Greek symbol

δ Liquid film thickness between wall and bubble, m

μ Dynamic viscosity, $N \cdot s/m^2$

ρ Density, kg/m^3

σ Coefficient of surface tension, N/m

$\vec{v}$ Velocity vector, m/s

Ω Volume fraction, (-)

Δt Time step size , sec

Δx Length interval, m

Subscript

L Liquid

G Gas

Superscript

T Transpose

Chapter-1

Introduction

Now-a-days for past processing of electronic devices we are using high processors that lead to more heat generation in the devices. As the heat generation increases the performance of the devices decreases. So the main objective is to remove heat from the devices without disturbing the performance of the devices. We can remove heat by using different methods like heat exchangers and etc., but the electronic devices are very small. So for the small devices we can use microchannels as the heat removing devices.

Microchannels, the devices which are having the diameter less than 0.2 mm and greater than 0.001 mm, have the great capability of removing heat by using fluid flow. Fluid flow can be single phase flow or two phase flow or multi-phase flow. In single phase flow there will be one fluid is flowing. Two phase flow is of different types. They are Gas-Liquid flows, Gas-Solid flows, Liquid-Liquid flows and Liquid-Solid flows. Multi-phase flow is the flow with more than two fluids.

Two-phase flow in microchannels has wide range of applications in micro scale heat transfer enhancement, biomedicine, microfiltration, and controlled drug delivery etc. to name a few. When liquid and gas, or two different immiscible fluids flow inside a small channel (e.g. T-shaped micro channels) different flow patterns based on the geometries, flow rates and the properties of the two fluids are created. The different patterns produced in two phase flow in microchannels are churn flow, bubble flow, annular flow, Taylor bubble or slug flow

Churn flow:

It refers as semi-annular flow or froth flow. Churn flow is defined as the flow with highly disturbed flow of liquid and gas. It can be described by the presence of very thick and unstable liquid film, with the liquid fluctuates up and down. Churn flow appeared only in vertical channels or nearly vertical channels.

Bubble flow:

In a liquid continuum if the small bubbles are dispersed or suspended as a discrete particle then the flow is called “Bubble flow”. The main feature of the bubble flow is that moving and deformable interfaces of bubbles in time as well as space domains and complex interactions in between the interfaces, and also between the liquid flow and the bubbles.

Annular flow:

In a gas-liquid two phase flow in microchannels if the liquid flows near the channel wall and the gas flows at the center of the channel as a gas flow core then the flow is called as "Annular flow". The gas flow core contains appropriated liquid droplets. Annular flow occurs when the light weight fluid is moving at the high velocities. This flow will appear in both vertical and horizontal channels.

Taylor bubble flow:

Taylor bubble flow is a liquid-gas flow pattern consisting of elongated bubbles separated by liquid slugs [1]. In Taylor bubble flow elongation of bubbles will be more than the channel diameter. The bubbles normally completely or almost completely fill the cross-section of the channel and a very thin liquid film separates the channel wall from the gas bubble. Taylor bubble flow can also be called as "slug flow".

Generally in two phase flow the rate of heat transfer is nearly twice that of the single phase flow. So we consider Taylor bubble flow, which is one of the flow patterns of two phase flow as discussed above, in microchannels. Because Taylor bubble flow in microchannels will have major applications in removing the heat and in other fields. Generally, Taylor bubble flow can be created by using a T-junction [2], Y-junction [3], or a concentric passage [4] where gas and liquid flow through two inlet passages which are concentric and meet inside the channel. Taylor bubble flow is the best desired flow pattern for micro bubble production in T-shaped micro channel.

Bubbles will form and flow when the gas enters at very low flow rate into a liquid flowing channel. As the gas flow rate increases up to certain value such that the diameter of the bubble exceeds the channel diameter, it will results in the elongated gas bubbles separated by liquid slugs, called Taylor bubble flow or Slug flow. The most commonly used microchannel geometry for creating Taylor bubble flow is a T-junction. Garstecki et al. [2] described the process of formation of bubbles in microfluidic T-junction geometries.

Generally in steady flows, the disturbance can be created by keeping an obstacle along the fluid flow. This will create the turbulence near the obstacle. In turbulent flow the rate of heat transfer is more when compared to the steady flow. So we consider an obstacle in the Taylor bubble flow in the microchannel such that it may raise the hope to enhance heat and mass transfer in the microchannels.

Chapter –2

Literature Review

The earliest study on Taylor bubbles was started a century ago when Gibson [5] studied the motion of air bubbles rising up in a vertical tube. Later on many researchers focused on understanding the hydrodynamics of Taylor bubble flow. With the emergence of micromanufacturing technology, many applications dealing with Taylor bubble flow emerged with time. This motivated researchers to relook at Taylor bubble flow in microchannel systems. Taylor bubble flow is predominantly found in small diameter channels where surface tension forces dominant the gravitational force.

Fairbrothers and Stubs [6] were the first to start the study on this kind of flows. They experimentally determined the liquid flow rate inside a capillary by movement of an indicator bubble and confirmed that a liquid thin film in between the bubble and tube wall which was the main reason for higher velocity of the bubble compared to that of the liquid. Taylor [7] conducted fair brother's experiments over a wide range of capillary numbers and for the reported values of relative bubble velocity. Triplett et al. [8] studied the air-water two phase flows through circular channel of 1.1 and 1.45 mm and semi-triangular channel of 1.09 and 1.49 mm hydraulic diameter experimentally. They observed bubbly, churn, slug, slug-annular and annular flow pattern. They also developed the flow pattern map using gas and liquid superficial velocity.

Kishimoto and Sasaki [9] used the concept to enhance heat transfer in microchannels where they used diamond shaped micro pin fins with staggered arrangement.

Zhao et al. [10] studied the co-current upward air-water two phase flow through triangular channel of 2.886, 1.433 and 0.866 mm hydraulic diameter experimentally and developed the flow pattern map. They observed the new flow pattern named capillary bubbly flow. They also observed that transition from slug to churn and churn to annular shifted towards right side in flow pattern map as hydraulic diameter decreases.

Liu et al. [11] studied the hydrodynamics of gas-liquid two phase flow through vertical circular mini channel of 0.91, 2 and 3.02 mm and vertical square of 0.99 and 2.89 mm hydraulic diameter. They investigated Taylor slug flow and the influence of liquid properties

on Taylor bubble rise velocity using water, ethanol and oil as liquid phase while air as gas phase.

Qian and lawal [12] numerically studied gas-liquid Taylor bubble flow in a microchannel, with varying cross-sectional width (0.25, 0.5, 0.75, 1, 2 and 3 mm). Thy obtained different gas and liquid slug lengths at different flow conditions and found to be in line with existing literature. They also developed correlation in T-junction microchannel based on the numerical simulation.

Baroud et al. [13] presented a state of the art of droplet formation, their transport and merger of drops in microfluidics and discussed issues related to effects of channel dimension, viscosity of fluid, and relative flow rate of the immiscible fluids used. One theory is that the slug or Taylor flow breaks into separate bubbles due to the pressure difference across the slug breaking neck, called squeezing effect. At low capillary numbers, the interfacial tension is strong compared to viscous stress. As the droplet grows, it blocks the channel, thus restricting the flow of continuous phase around it. So, stable parallel dispersed micro bubbles are created in this regime. When the capillary number is high, the droplets are released before they actually block the channel and their formation is entirely due to the action of shear stress.

Santos and kawaji [14] both numerically and experimentally studied two-phase flow using gas-liquid, and a microfluidic T-junction (nearly square microchannel, D_h = 113 μm). The estimation of slug flow through numerical simulation demonstrated that cfd codes can also accurately predict Taylor flow in microchannels.

Yang et al. [15] studied the effect of rheological properties of non-newtonian fluid on gas-non newtonian liquid two phase flow in vertical square and triangular of 0.866, 2.5 and 2.866 mm hydraulic diameter experimentally. They used carboxymethyle cellulose, polyacrylamide and xanthan gum as non-newtonian fluid whereas nitrogen as a gas phase. They developed flow pattern map for all cases.

Zhang et al. [16] conducted experiments on the horizontal microchannels with different channel diameter and the influence of liquid physical properties on the flow patterns in the channel are studied. They stated a new model which considers the effects of channel size and liquid physical properties is proposed. Three empirical correlations are proposed for predicting the transitions from slug to bubbly flow, from slug to churn and slug-annular flow, and from churn to slug-annular and annular flow, respectively.

Pham et al. [17] used volume-of-fluid (VOF) model foe numerical simulation of gas-liquid flows in a T-junction microchannel and predicted the pressure and velocity distribution, and phase of fluid in the microchannel.

Recently, Rubio-jimenez et al. [18] proposed micro pin fin heat sink with variable fin density in order to gradually increase the heat transfer coefficient while maintaining uniform surface temperature. Taylor flow enhances heat and/or mass transfer due to internal circulation inside the liquid plugs [19]. But once the Taylor bubble is formed, it hardly changes its shape when it flows through a straight horizontal microchannel.

Krepper et al. [20] demonstrated the complicated relationship and interference between size dependent bubble migration, bubble coalescence and breakup effects in two phase flows where they used the inhomogeneous MUSIG approach.

Majumder et al. [21] experimentally studied local thermal performance of square mini-channel with air-water Taylor bubble flow with an objective to study the heat transfer enhancement if any, compared to single phase thermally developing flows. They found that presence of bubble influence the local wall and bulk fluid temperature and the heat transfer enhance up to 1.2-1.6 times compared to single-phase laminar flow as Taylor bubble train flows past the observation region. Secondly, it is found that the length of adjacent gas bubble and water plug also influence the local heat transfer enhancement. The flow in microchannel systems is mostly laminar in nature due to very small hydraulic diameter and lower flow rate. Conventionally, turbulent flow causes mixing of fluids, and hence higher heat transfer. Waves are formed as fluid flows past any structure, and creates turbulence. In recent times, pin fins are used as micro structures over plane microchannel wall to increase heat transfer surface area, and create mixing and turbulence; hence enhance heat transfer compared to plane rectangular microchannels.

The work by Kishimoto and Sasaki [9], and Rubio-jimenez et al. [18], Thulasidas et al. [19] and Majumder et al. [21] motivated to consider combining the concept of pin-fin with Taylor bubble flow and verify the thermal performance characteristics of microchannels under such condition. Under this background a numerical study is undertaken to study hydrodynamics of Taylor bubble as it flows past an obstacle placed inside a microchannel. In this work an obstacle (square in shape) is placed inside the microchannel with an expectation to create disturbance to the gas-fluid interface of Taylor bubble and thus affect the flow pattern. The effect of the obstacle positions (along the cross sectional area of the microchannel) on the flow pattern has been studied.

Chapter –3

Numerical simulation

3.1. Problem Description:

In this work a two-dimensional numerical study has been carried out to study the hydrodynamics of Taylor bubble as it flows past an obstacle placed inside a microchannel and heat transfer comparison for single phase flow and two phase flow in microchannel without obstacle is done with two different metals namely aluminum and steel.

A T-junction is used to create Taylor bubble by allowing water and air to enter at two inlets of a T-junction as shown in Fig. 3.1. The width and length of the main channel are 0.2 mm and 4.5 mm respectively. The length of the water liquid inlet and air inlet are 1 mm and 0.5 mm respectively. An obstacle (square in shape and 0.02×0.02 mm^2 in size) is placed at a distance of 2 mm from the T-junction as shown in Fig. 3.1. The position of the obstacle is varied by moving it along the perpendicular to the fluid flow direction indicated by "y", the distance of the obstacle center from the right wall, as shown in Fig. 3.1. The rate of heat transfer for the water-air two phase flow in microchannel with an obstacle at the center of the channel has been studied. Here we refer as left and right side to indicate the space/gap above and below the obstacle shown in Fig. 3.1.

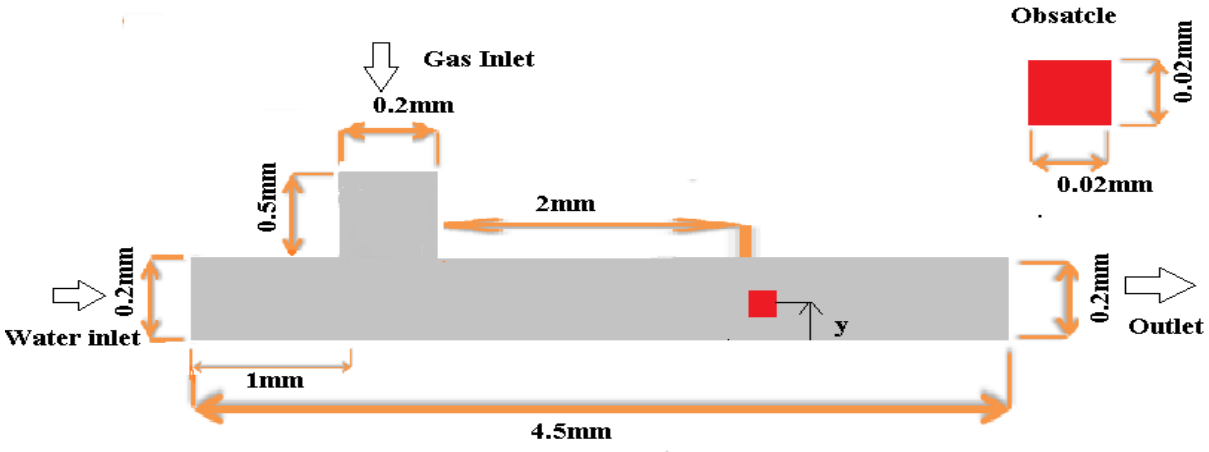

Figure 3.1: Top view of T-section for creating Taylor bubble flow with an obstacle.

3.1.1. Positions of obstacle:

The position of the obstacle is defined by the distance between the center of the obstacle and the right wall of the microchannel which is varied in steps of 0.02 from maximum value of 0.1 mm to minimum value of zero.

At y = 0.1 mm:

In this case the obstacle is placed at the center of the microchannel, i.e. the obstacle stays at a distance of 0.9 mm from the both walls of the microchannel.

At y = 0.08 mm:

In this case the obstacle is moved towards the right side of the channel with a distance of 0.02 mm, i.e. the obstacle stays at a distance of 0.11 mm and 0.07 mm from left and right wall of the channel respectively.

At y = 0.06 mm:

The center of the obstacle is placed at a distance of 0.06 mm from the right wall of the channel, i.e. the obstacle stays at a distance of 0.13 mm and 0.05 mm from left and right side of the channel respectively.

At y = 0.04 mm:

In this case the obstacle stays at a distance of 0.15 mm and 0.03 mm from left and right wall of the channel respectively. The obstacle center is at a distance of 0.04 mm from the right wall of the channel.

At y = 0.02 mm:

The center of the obstacle is placed at a distance of 0.02 mm from the right side wall of the channel, i.e. the obstacle stays at a distance of 0.17 mm and 0.01 mm from left and right wall of the channel respectively.

At y = 0 mm:

The center of the obstacle is kept on the right wall of the channel, i.e. only half of the obstacle is placed inside the channel. So the obstacle size in this case is half of the obstacle size compared to previous cases.

Initially the main channel was filled with water and the side channel with air, and the air and water were fed in to the channel at different constant velocity. The fluid (both air and water) flow is considered laminar at the inlet. Water velocity at the inlet is set at 0.251 m/s (Re = 50). Fully developed velocity profile at the inlet is considered by using user defined function (UDF). Air velocity at the inlet is considered to be 0.073m/s (Re = 1).

3.2. Governing Equations:

The Courant number can be defined as

$$C = \Delta t \sum_{i=1}^{n} \frac{u_{x_i}}{\Delta x_i} \tag{1}$$

where u is the magnitude of the velocity, ΔT is the time step size, Δx is the length interval. The governing equations of the volume of fluid (VOF) formulations on multiphase flow are as follows:

Equation of continuity:

$$\left(\partial\rho / \partial t\right) + \nabla.\left(\rho\vec{v}\right) = 0 \tag{2}$$

Equation of motion:

$$\frac{\partial\left(\rho\vec{v}\right)}{\partial t} + \nabla.\left(\rho\vec{v}\vec{v}\right) = -\nabla p + \nabla.\left[\mu\left(\nabla\vec{v} + \nabla\vec{v}^{T}\right)\right] + \vec{F} \tag{3}$$

where ρ is density, t is time, p is pressure, $\vec{v}$ is velocity vector, μ is dynamic viscosity, $\vec{F}$ is surface tension force of the fluid. The superscript T indicates transpose.

Volume fraction equation:

$$\frac{\partial\Omega_G}{\partial t} + \vec{v}.\nabla\Omega_G = 0 \tag{4}$$

$$\rho = \Omega_G\rho_G + \left(1-\Omega_G\right)\rho_L \tag{5}$$

$$\mu = \Omega_G\mu_G + \left(1-\Omega_G\right)\mu_L \tag{6}$$

where Ω_G is volume fraction of gas, ρ is density and μ is dynamic viscosity. The subscript L and G indicate for liquid (water) and gas (air) respectively.

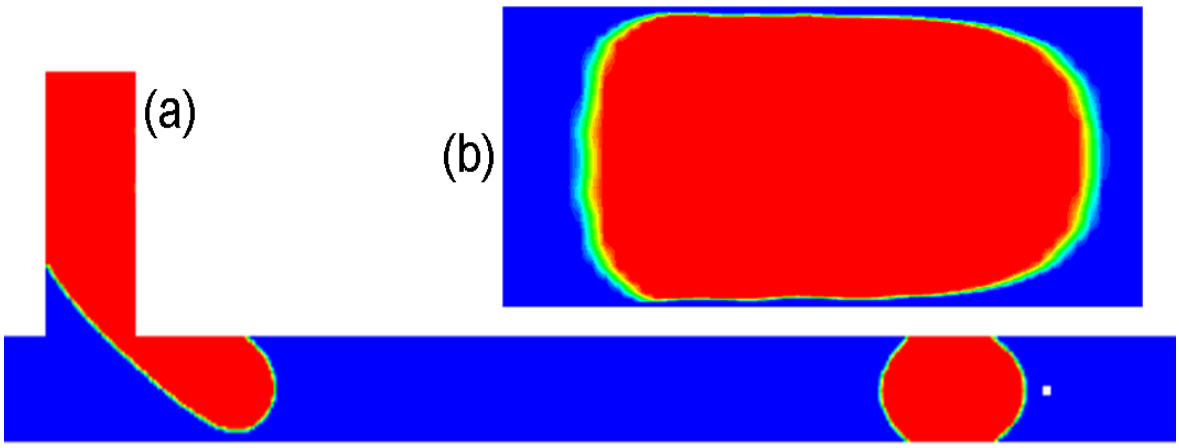

Figure 3.3: (a) Taylor bubble flow in T-section (b) zoom view of a bubble with liquid film thickness captured near the wall.

At low capillary numbers ($Ca < 10^{-2}$) interfacial tension dominates the viscous stress that leads to the formation of bubbles in the microchannels. For higher values of capillary number viscous stress is stronger than the interfacial tension that leads to the formation of continuous flow (annular flow). The capillary number is defined as

$$Ca = \frac{\mu_L (v_L + v_G)}{\sigma} \tag{7}$$

where μ_L is the viscosity of the water, v_L is the velocity of water and v_G velocity of air, σ is the coefficient of surface tension [22]. Bretherton [23] proposed correlation for liquid film thickness (δ) given by

$$\delta = 1.34R \cdot Ca^{2/3} \tag{8}$$

where R is the channel radius. To capture the film thickness numerically, one require considering fine meshing near the wall such that appreciable number of mesh is placed inside the boundary layer.

Based on their numerical simulation results, Gupta et al. [22] proposed to consider a minimum of five nodes across the liquid film thickness (δ) i.e. from the wall up to a distance.

3.3. Numerical Analysis:

The general approach for the modeling of multiphase flow in microchannels is to compute the evolution of the gas-liquid interface. In order to capture the interface between the gas and liquid, one of the basic multiphase models in Ansys Fluent®, the Volume-of-Fluid (VOF) model is used to simulate gas – liquid flows in the T-junction microchannel.

Different multiphase models available are (i) Volume-of-Fluid (VOF) model, (ii) Mixture model, (iii) Eulerian model). The VOF model is the only model that can capture the liquid-gas interface clearly. The VOF model is applicable for two or more immiscible fluids.

Iterative time advancement pressure based unsteady solver is used in the fluent. Two fluids used are air and water liquid. The Volume-of–Fluid (VOF) model is used in this problem to identify the interface between water liquid and air. Air is set as primary phase and water is set as secondary phase. The interface is in a good accordance with the chosen contact angle of 36^o. Surface tension coefficient was set to 0.0735 N/m and wall adhesion is considered [17]. The mesh size is 0.005mm in this study. The fluid flow is considered laminar at the inlet. Inlet velocity of liquid water and air are set as 0.251 m/s (Re = 50) and

0.073 m/s (Re = 1) respectively. Fully developed velocity profile at the inlet is considered by taking user defined function (UDF).

For pressure discretization PRESTO scheme is used. The PISO scheme is used for pressure–velocity coupling, second order upwind scheme used for discretization associated with momentum equation, the geometric reconstruction scheme used for interface interpolation, and implicit body force treatment for body force formulation. The convergence criteria are set to 1×10^{-6} for continuity and x-velocity residuals, and 1×10^{-8} for y-velocity residual.

The main control over the time-stepping scheme is the Courant number (CFL). The time step is proportional to the CFL. Thus the global courant number is set to 0.25 and the maximum and minimum time step size is set as 10^{-4} and 10^{-8} sec respectively for calculation of the volume fraction. Additionally, the maximum number of iterations per time step is set to 20.

Chapter –4

Results and Discussion

Figure 3.1 shows T-junction arrangement that us used for forming Taylor bubble which is shown in Fig. 3.3. For the flow parameters considered in this study (Re_L = 50, Re_G = 1), the length of the bubble is found to be slightly bigger than the diameter of the channel. Re_L indicates Reynolds number of liquid (water) at the inlet of the microchannel, Re_G indicates Reynolds number of gas (air) at the side inlet. Figure 3.3(b) shows the zoom view of a Taylor bubble that shows very thin liquid film captured near the wall with proper selection of grid size near the wall. A grid independence test is carried out to find the suitable grid size for the geometry and the parameters considered in this study. An obstacle is positioned inside the channel at the downstream. The position of the obstacle is decided such that the bubble stabilizes after leaving the T-junction by the time it reaches near the obstacle. The obstacle position is varied along the cross section of the microchannel with perpendicular to the fluid flow direction.

As discussed in the chapter 3, seven different cases has been considered and studied successfully. Phase contours, velocity vectors, and required plots have been produced for all the cases. The most efficient results for the above cases are mentioned below.

Taylor bubble flow pattern for different obstacle position:

The position of the obstacle is defined by the distance of the center of the obstacle from the nearby right wall denoted as y as shown in Fig. 3.1. The position of the obstacle varied between exactly at center (y is maximum i.e. 0.1 mm) and the obstacle is part of the wall (y is minimum i.e. zero).

4.1. Obstacle positioned at y = 0.1 mm:

First the obstacle is placed exactly at the center of the channel such that y = 0.1. In such case there will be equal space of 0.09 mm each on the both sides of the obstacle through which the fluid can flow. The sequence of images showing flow of one air bubble past an

obstacle is presented in Fig. 4.1. The time lag between two consecutive snaps is approximately 70 μ-secs.

Just before the Taylor bubble is about to touch, it is symmetric in shape, the obstacle as can be seen in Fig 4.1(a). The tip of the Taylor bubble will first touch the obstacle as it is placed exactly at the center of the channel. The phase contour for this moment is not shown here, it will come in between the sequence of Fig. 4.1(b) and 4.1(c). When Taylor bubble touches this obstacle, it splits in to two and starts moving through both sides of the obstacle, with perfect symmetric flow, as shown in Fig. 4.1(c-e). Once split, two tips of the bubble are formed on either side of the obstacle. Once the bubble starts advancing, and travels a distance approximately equal to the gap on either side (i.e. 0.09 mm), it starts to expand towards the center of the channel from either side of the obstacle. Immediately, the two parts of the bubble touch each other nearly half the gap i.e. 0.045 mm away from the obstacle at a downstream location. This moment is not reported here, which will come in between Fig. 4.1(e) and 4.1(f). So, the two parts join to form the original bubble as it moves past the obstacle. For some time, the obstacle will be surrounded by the bubble only, as can be seen in Fig. 4.1(f-l). Also a small amount of water will be trapped behind the obstacle. This is due to merging of two parts of the bubble at a distance away from the obstacle in the downstream location. This is in line with the prior expectation. As the rear meniscus touches the obstacle, it again gets divided in to two parts due to presence of some water at the backside of the obstacle. This can be seen in Fig. 4.1(m). Soon, the rear meniscus tries to regain its original shape (minimize the length of the rear meniscus arc) and it again comes in contact with the back side of the obstacle. As the bubble moves forward, it tries to snatch it from the obstacle and in the process a tail will elongate between the bubble and the back face of the obstacle. This can be observed in Fig. 4.1(n-o). This will continue for a while till it moves some sufficient distance that force it to snatch away from the obstacle (see Fig. 4.1(p)). As soon as the rear meniscus of the bubble gets detached from the obstacle, it again tries to regain its original shape (see Fig. 4.1(p-q)) and in a while comes to its original shape and size (see Fig. 4.1(r.))).

During its journey of the bubble from the position shown in Fig. 4.1(a) to 4.1(r) as it flows past an obstacle, the shape of the air-water interface continuously changing, thus the water near the bubble interface also continuously changing its position with respect to the wall. This causes rapid mixing compared to a Taylor bubble flow in a microchannel without any obstacle. This creates turbulence it may leads to more heat transfer.

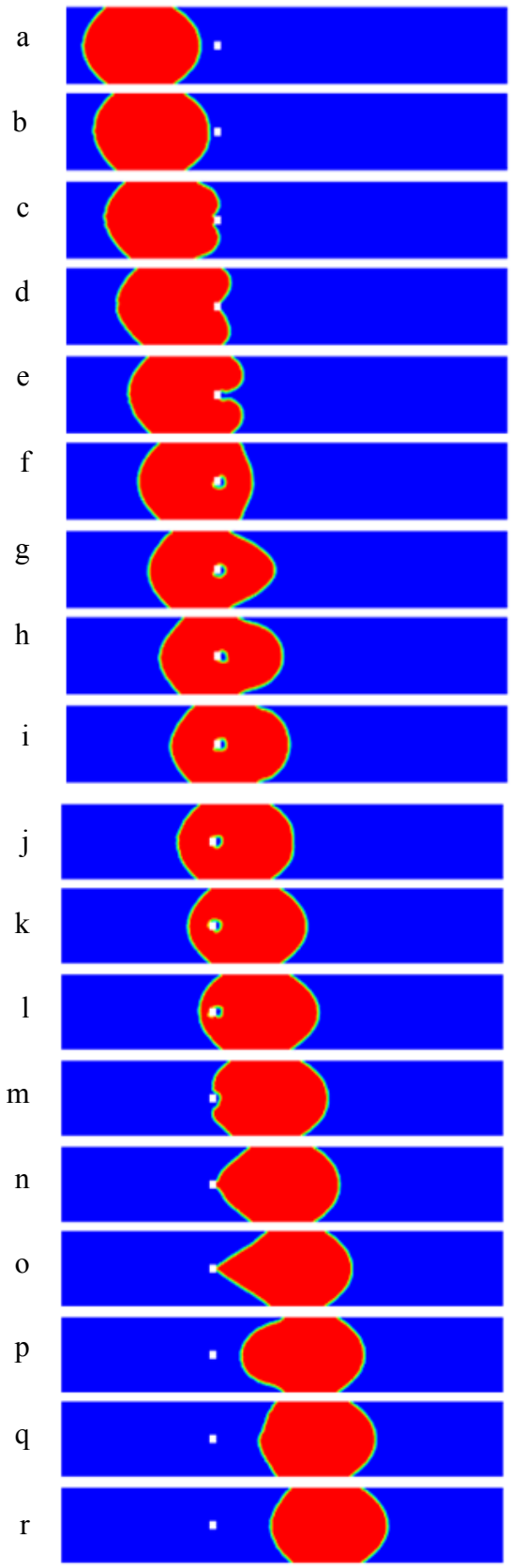

Figure 4.1: Taylor bubble crosses the obstacle positioned at y = 0.1 (center).

4.2. Obstacle positioned at y = 0.08 mm:

Figure 4.2 presents the sequence of images showing flow of one air bubble past an obstacle when y = 0.08. Because of the position of the obstacle, the front meniscus of the bubble will touch the obstacle at a point towards the right side of the tip. This is shown in Fig. 4.2(b). Now, as the bubble touches the obstacle the front meniscus of bubble moves forward from both the left side and the right side portion of the obstacle and start to develop two independent meniscuses and try to obtain the similar shape of the parent bubble shape before hitting the obstacle. The left side portion of the front meniscus tries to move forward continuously while the right side portion of this meniscus will move forward up to some extent only. After that the right side portion of the front meniscus doesn't move further. This can be viewed by comparing Fig. 4.2(c) and Fig. 4.2(d). As the left side portion of the front meniscus continuously move forward it grows simultaneously towards the right side of the obstacle such that its shape should be of a circular arc passes through the obstacle and its contact point on the left side wall. In this process, the contact point on the left wall slowly moves forward and the radius of the circular arc continuously grow till the meniscus touches down at the right wall. This can be observed in Fig. 4.2(i). During this process, due to the expansion of bubble towards the right side of the obstacle a small amount of water starts moving backward and it pushes the water present below the obstacle. The contact point of right portion of the front meniscus with the right wall slowly moves backward, thus the front right meniscus starts getting flattened between the obstacle and the continuously (backward) moving contact point on the right wall. In the meantime the back meniscus is continuously moving forward along with the contact point of this meniscus with the right wall. This can be seen from Fig. 4.2(f-g). After a while the two contact points (front meniscus and rear meniscus) on the right wall meet at a common point, which can be seen in Fig. 4.2(h).

When the bubble (rear and the front right meniscus) gets detached from the right wall, together they (rear and the front right meniscus) try to form a circular arc shape. This can be seen in Fig. 4.2(i-j). Normally, the lift up and detachment order will depend on the length of the bubble along the channel. In this case the lift up takes place first at the right side portion of the right front meniscus, then followed by the touch down at the right side portion of the left front meniscus. This is due to smaller length of the bubble (of the order of the channel

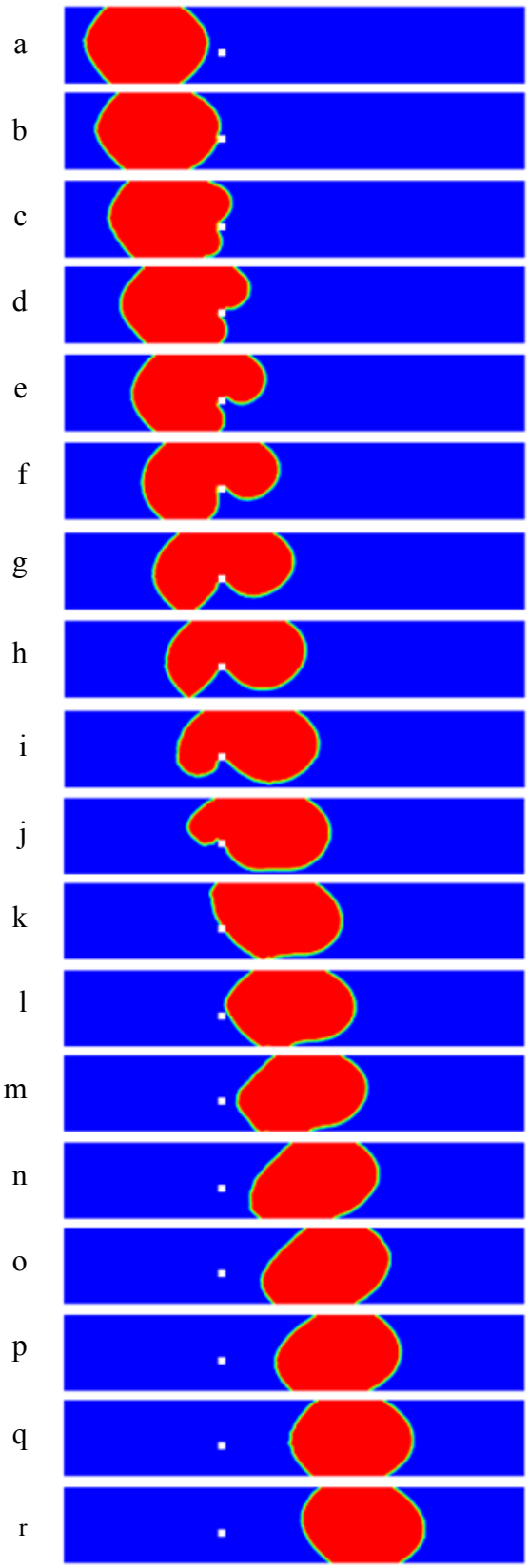

Figure 4.2: Taylor bubble crosses the obstacle positioned at y = 0.08.

width). For longer length of the bubble, the touchdown will take place first, followed by lift up. Next, when the back meniscus leaves the obstacle, the effect of snatching can be observed, which makes a V-shaped or tail-shaped back meniscus (for a while (see Fig. 4.2(l-m)) due to flattening of the left and the right portion of the back meniscus. After this moment, the bubble tries to return to its original shape in a while, where the tip of the front meniscus continuously moves towards the center and the tip of the back meniscus continuously moves towards the center.

4.3. Obstacle positioned at y = 0.06 mm:

Figure 4.3 presents the sequence of images showing flow of one air bubble past an obstacle when y = 0.06. Thus, the gap on the left and the right side will be equal to 0.13 mm and 0.05 mm respectively. Because of the position of the obstacle, the front meniscus will touch the obstacle at a point towards the right side of the tip. This can be seen in Fig. 4.3(b). Now, as the bubble touches the obstacle the front meniscus of bubble moves forward from both the left side and the right side portion of the obstacle and start to develop two independent meniscuses and try to obtain the similar shape of the parent bubble shape before hitting the obstacle. The left side portion of the front meniscus tries to move forward continuously while the right side portion of this meniscus will move forward up to some extent only. After that the right side portion of the front meniscus doesn't move further. This can be viewed by comparing Fig. 4.3(c) and Fig. 4.3(d). As the left side portion of the front meniscus continuously move forward it grows simultaneously towards the right side of the obstacle such that its shape should be of a circular arc passes through the obstacle and its contact point on the left side wall. In this process, the contact point on the left wall slowly moves forward and the radius of the circular arc continuously grow till the meniscus touches down at the right wall. This can be observed in Fig. 4.3(i). During this process, due to the expansion of bubble towards the right side of the obstacle a small amount of water starts moving backward and it pushes the water present below the obstacle. The contact point of right portion of the front meniscus with the right wall slowly moves backward, thus the front right meniscus starts getting flattened between the obstacle and the continuously (backward) moving contact point on the right wall. In the meantime the back meniscus is continuously moving forward along with the contact point of this meniscus with the right wall. This can be seen from Fig. 4.3(f-g). After a while the two contact points (front meniscus and rear meniscus) on the right wall meet at a common point, which can be seen in Fig. 4.3(h).

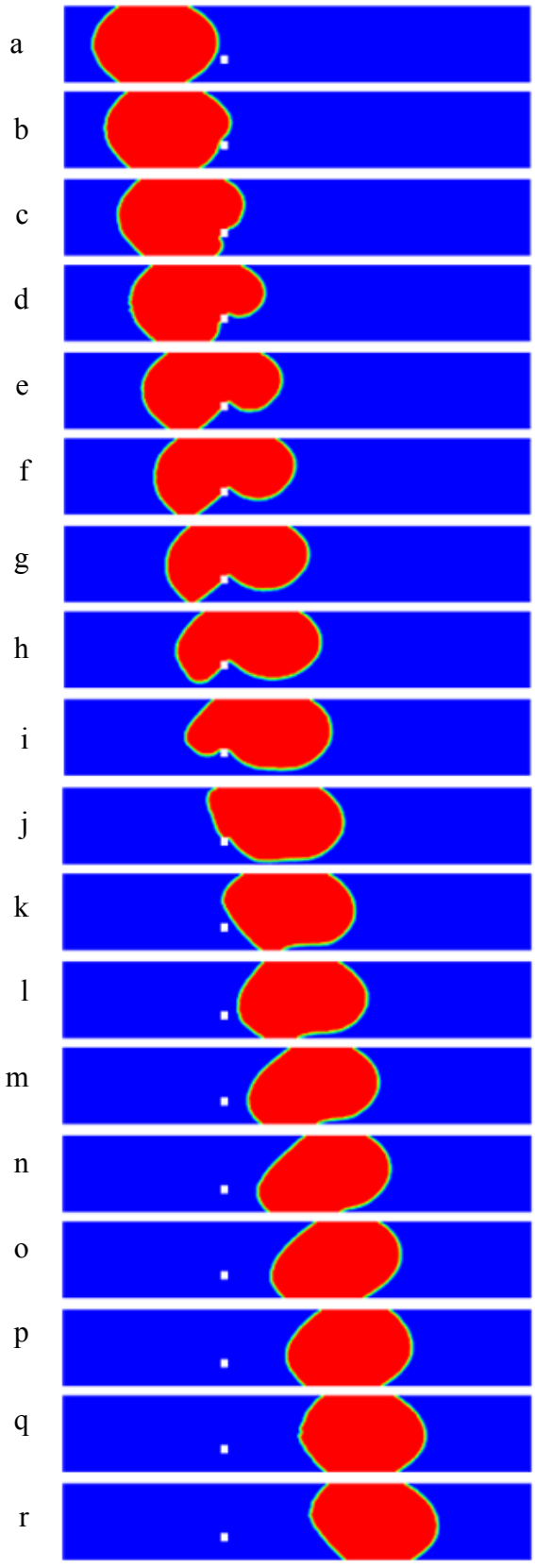

Figure 4.3: Taylor bubble crosses the obstacle positioned at y = 0.06 mm.

When the bubble (rear and the front right meniscus) gets detached from the right wall, together they (rear and the front right meniscus) try to form a circular arc shape. This can be seen in Fig. 4.3(i-j). Normally, the lift up and detachment order will depend on the length of the bubble along the channel. In this case the lift up takes place first at the right side portion of the right front meniscus, then followed by the touch down at the right side portion of the left front meniscus. This is due to smaller length of the bubble (of the order of the channel width). For longer length of the bubble, the touchdown will take place first, followed by lift up. Next, when the back meniscus leaves the obstacle, the effect of snatching can be observed, which makes a V-shaped or tail-shaped back meniscus (for a while (see Fig. 4.3(l-m)) due to flattening of the left and the right portion of the back meniscus. After this moment, the bubble tries to return to its original shape in a while, where the tip of the front meniscus continuously moves towards the center and the tip of the back meniscus continuously moves towards the center.

4.4. Obstacle positioned at y = 0.04 mm:

Figure 4.4 presents the sequence of images showing flow of one air bubble past an obstacle when y = 0.04. For this position of the obstacle, there will be a gap of 0.03 mm one side, and 0.15 mm on the other side of the obstacle. Here we refer as left and right side to indicate the space/gap above and below the obstacle shown in Fig 3.1. Thus, the gap on the left and the right side will be equal to 0.15 mm and 0.03 mm respectively. Because of the position of the obstacle, the front meniscus will touch the obstacle at a point towards the right side of the tip. This can be seen in Fig. 4.4(b). Now, as the bubble touches the obstacle the front meniscus of bubble moves forward from the left side portion of the obstacle and start to develop an independent meniscus and try to obtain the similar shape of the parent bubble shape before hitting the obstacle. The right side portion of the front meniscus tries to move forward continuously while the right side portion of this meniscus will move forward up to some extent only. After that the right side portion of the front meniscus doesn't move further. This can be viewed by comparing Fig. 4.4(c) and Fig. 4.4(d). As the left side portion of the front meniscus continuously move forward it grows simultaneously towards the right side of the obstacle such that its shape should be of a circular arc passes through the obstacle and its contact point on the left side wall. In this process, the contact point on the left wall slowly moves forward and the radius of the circular arc continuously grow till the meniscus touches down at the right wall. This can be observed in Fig. 4.4(k). During this process, due to the expansion of bubble towards the right side of the obstacle a small amount of water starts

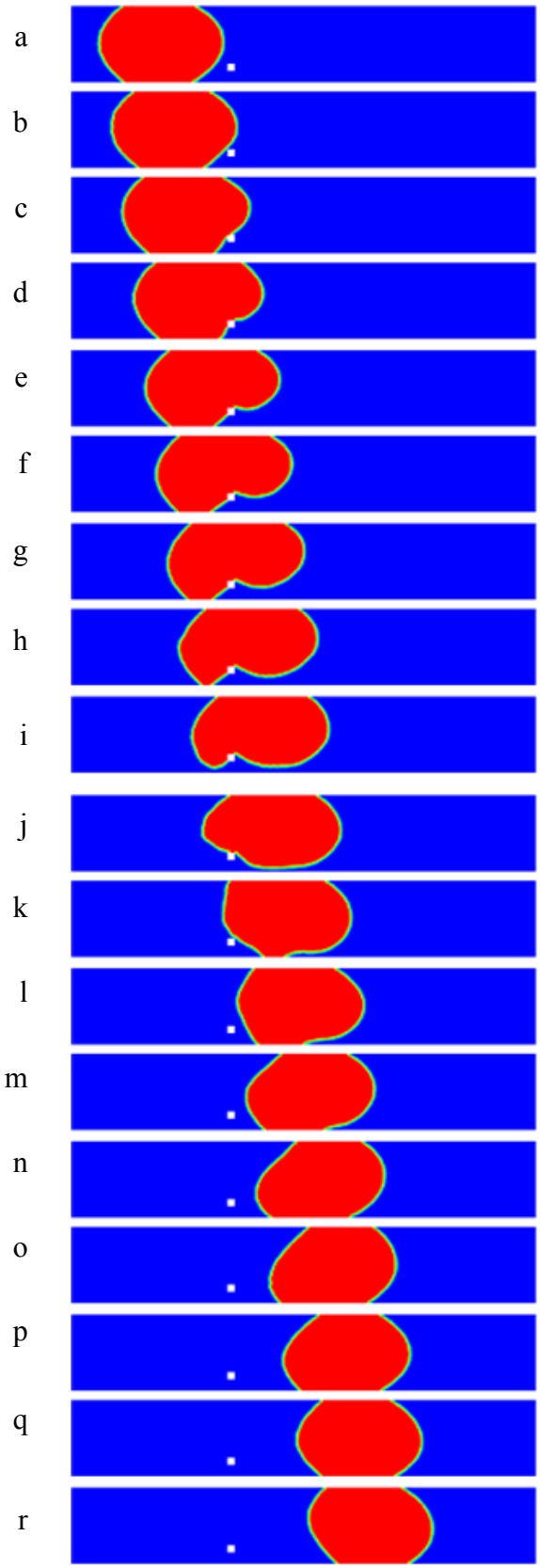

Figure 4.4: Taylor bubble crosses the obstacle positioned at y = 0.04 mm.

moving backward and it pushes the water present below the obstacle. The contact point of right portion of the front meniscus with the right wall slowly moves backward, thus the front right meniscus starts getting flattened between the obstacle and the continuously (backward) moving contact point on the right wall. In the meantime the back meniscus is continuously moving forward along with the contact point of this meniscus with the right wall. This can be seen from Fig. 4.4(e-g). After a while the two contact points (front meniscus and rear meniscus) on the right wall meet at a common point, which can be seen in Fig. 4.4(h).When the bubble (rear and the front right meniscus) gets detached from the right wall, together they (rear and the front right meniscus) try to form a circular arc shape. This can be seen in Fig. 4.4(i-j). Normally, the lift up and detachment order will depend on the length of the bubble along the channel. In this case the lift up takes place first at the right side portion of the right front meniscus, then followed by the touch down at the right side portion of the left front meniscus. This is due to smaller length of the bubble (of the order of the channel width). For longer length of the bubble, the touchdown will take place first, followed by lift up. Next, when the back meniscus leaves the obstacle, the effect of snatching can be observed, which makes a V-shaped or tail-shaped back meniscus (for a while (see Fig. 4.4(l-m)) due to flattening of the left and the right portion of the back meniscus. After this moment, the bubble tries to return to its original shape in a while, where the tip of the front meniscus continuously moves towards the center and the tip of the back meniscus continuously moves towards the center.

4.5. Obstacle positioned at y = 0.02 mm:

Figure 4.5 presents the sequence of images showing flow of one air bubble past an obstacle when y = 0.02. For this position of the obstacle, there will be a gap of 0.01 mm one side, and 0.17 mm on the other side of the obstacle. Because of the position of the obstacle, the front meniscus will touch the obstacle at a point towards the right side of the tip. This can be seen in Fig. 4.5(b). Now, as the bubble touches the obstacle the front meniscus of bubble moves forward from the left side portion of the obstacle and start to develop an independent meniscus and try to obtain the similar shape of the parent bubble shape before hitting the obstacle. The right side portion of the front meniscus tries to move forward continuously while the right side portion of this meniscus will move forward up to some extent only. After that the right side portion of the front meniscus doesn't move further. This can be viewed by comparing Fig. 4.5(c) and Fig. 4.5(d). As the left side portion of the front meniscus continuously move forward it grows simultaneously towards the right side of the obstacle

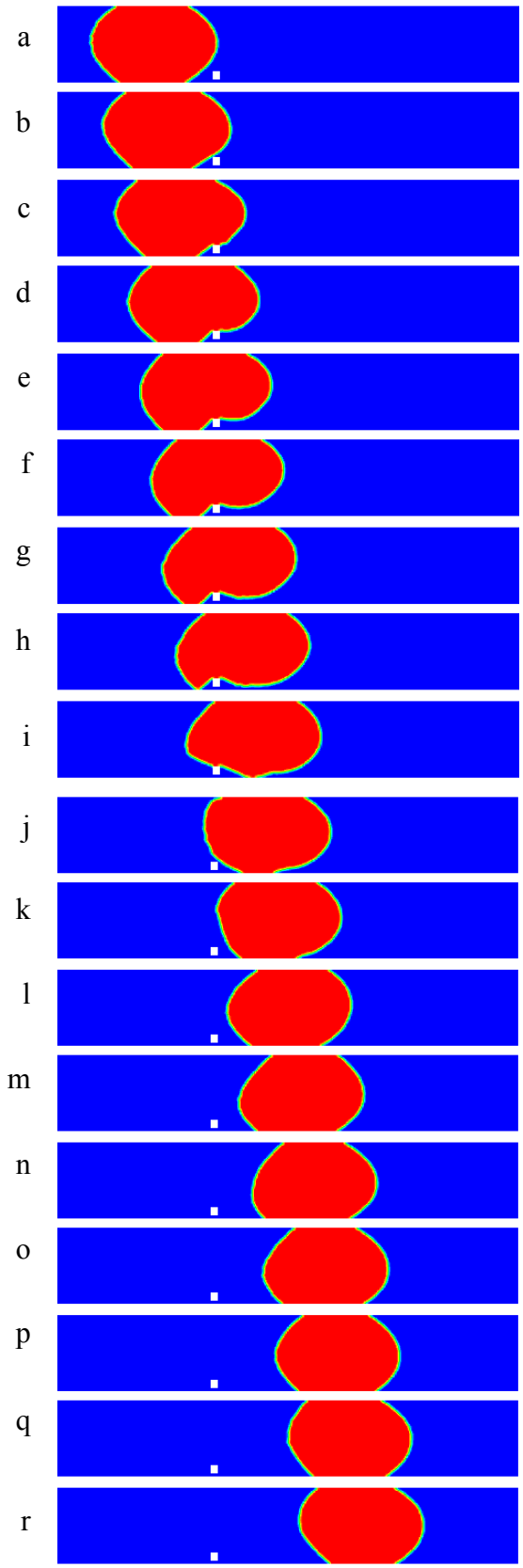

Figure 4.5: Taylor bubble crosses the obstacle positioned at y = 0.02 mm

such that its shape should be of a circular arc passes through the obstacle and its contact point on the left side wall. In this process, the contact point on the left wall slowly moves forward and the radius of the circular arc continuously grow till the meniscus touches down at the right wall. This can be observed in Fig. 4.5(i). During this process, due to the expansion of bubble towards the right side of the obstacle a small amount of water starts moving backward and it pushes the water present below the obstacle. The contact point of right portion of the front meniscus with the right wall slowly moves backward, thus the front right meniscus starts getting flattened between the obstacle and the continuously (backward) moving contact point on the right wall. In the meantime the back meniscus is continuously moving forward along with the contact point of this meniscus with the right wall. This can be seen from Fig. 4.5(f-g). After a while the two contact points (front meniscus and rear meniscus) on the right wall meet at a common point, which can be seen in Fig. 4.5(h).

When the bubble (rear and the front right meniscus) gets detached from the right wall, together they (rear and the front right meniscus) try to form a circular arc shape. This can be seen in Fig. 4.5(i-j). Normally, the lift up and detachment order will depends on the length of the bubble along the channel. In this case the lift up takes place first at the right side portion of the right front meniscus, then followed by the touch down at the right side portion of the left front meniscus. This is due to smaller length of the bubble (of the order of the channel width). For longer length of the bubble, the touchdown will take place first, followed by lift up. Next, when the back meniscus leaves the obstacle, the effect of snatching can be observed, which makes a V-shaped or tail-shaped back meniscus (for a while (see Fig. 4.5(l-m)) due to flattening of the left and the right portion of the back meniscus. After this moment, the bubble tries to return to its original shape in a while, where the tip of the front meniscus continuously moves towards the center and the tip of the back meniscus continuously moves towards the center.

4.6. Obstacle positioned at y = 0:

Figure 4.6 presents the sequence of images showing flow of one air bubble past an obstacle at y=0 i.e. the half of the obstacle is protruded into the microchannel. Because of the position of the obstacle, the front meniscus will touch the obstacle at a point towards the right side of the tip. This can be seen in Fig. 4.6(c). Now, as the bubble touches the obstacle the front meniscus of bubble moves forward from the left side portion of the obstacle and start to develop an independent meniscus and try to obtain the similar shape of the parent bubble

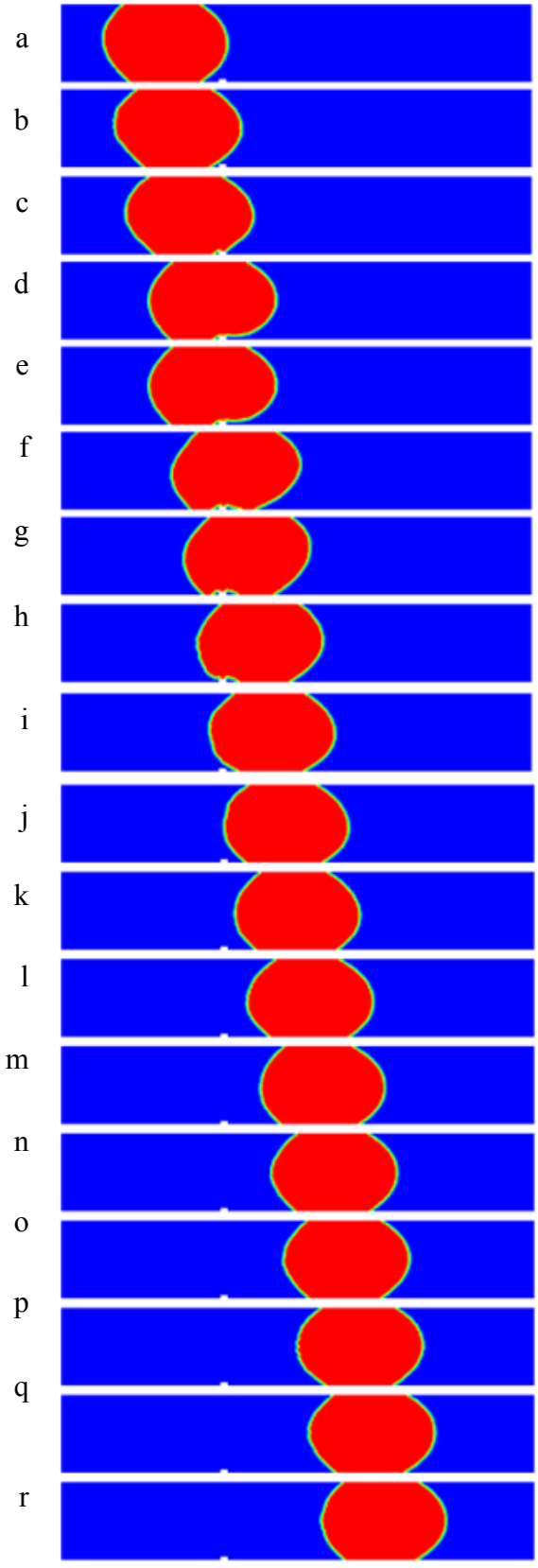

Figure 4.6: Taylor bubble crosses the obstacle positioned at y = 0 mm.

shape before hitting the obstacle. As the bubble touches the obstacle there will be some water is trapped in between the obstacle, right wall of the channel and the bubble. This can be

observed by comparing Fig. 4.6(d) and Fig. 4.6(e). Now the front left meniscus continuously move forward and also simultaneously grow towards the right such that it retains the shape of a circular arc passing through the obstacle and the contact point on the left side wall. In this process, the contact point on the left wall slowly moves forward and the radius of the circular arc of which the meniscus is a part, continuously grow till the meniscus touches down at the right wall. This can be observed in Fig. 4.6(f).

Here the water is trapped in between the obstacle, air bubble and the channel wall as shown in the Fig. 4.6(f-h). The contact point of the front meniscus with the obstacle slowly moves backward, thus the front meniscus before the obstacle starts getting flattened between the obstacle and the continuously (backward) moving contact point on the right wall. In the meantime the back meniscus is continuously moving forward along with the contact point of this meniscus with the right wall. This can be observed from Fig. 4.6(f-g). After a while the two contact points on the right wall meet at a common point, which can be seen in Fig. 4.6(g).

When the bubble (back and the front right meniscus) gets detached (lift up) from the right wall, together they (back and the front right meniscus) try to form a circular arc shape. This can be seen in Fig. 4.6(h-i). Normally, the lift up and detachment order will depend on the length of the bubble along the channel. In this case the lift up takes place first at the right side portion of the right front meniscus, then followed by the touch down at the right side portion of the left front meniscus. This is due to smaller length of the bubble (of the order of the channel width). For longer length of the bubble, the touchdown will take place first, followed by lift up. After this moment, the bubble tries to return to its original shape in a while, where the tip of the front meniscus continuously moves towards the center and the tip of the back meniscus continuously moves towards the center.

The velocity vectors indicate the direction of flow and the level of turbulence in any fluid flow region. Therefore the velocity vector diagram for different flow condition near the obstacle is present next. Figure 4.7 represents the velocity vector at four different regions of the microchannel

a) Velocity vector at a region where only liquid water is flowing inside a microchannel and there is no obstacle along the channel.
b) Velocity vector downstream of the obstacle (obstacle is at channel center) when only liquid water is flowing past the obstacle.
c) Velocity vector in front of the advancing meniscus of a Taylor bubble when it flows inside a microchannel without any obstacle.

d) Velocity vector in front of the advancing meniscus of the Taylor bubble when the Taylor bubble is flowing past an obstacle placed at the center of the channel.

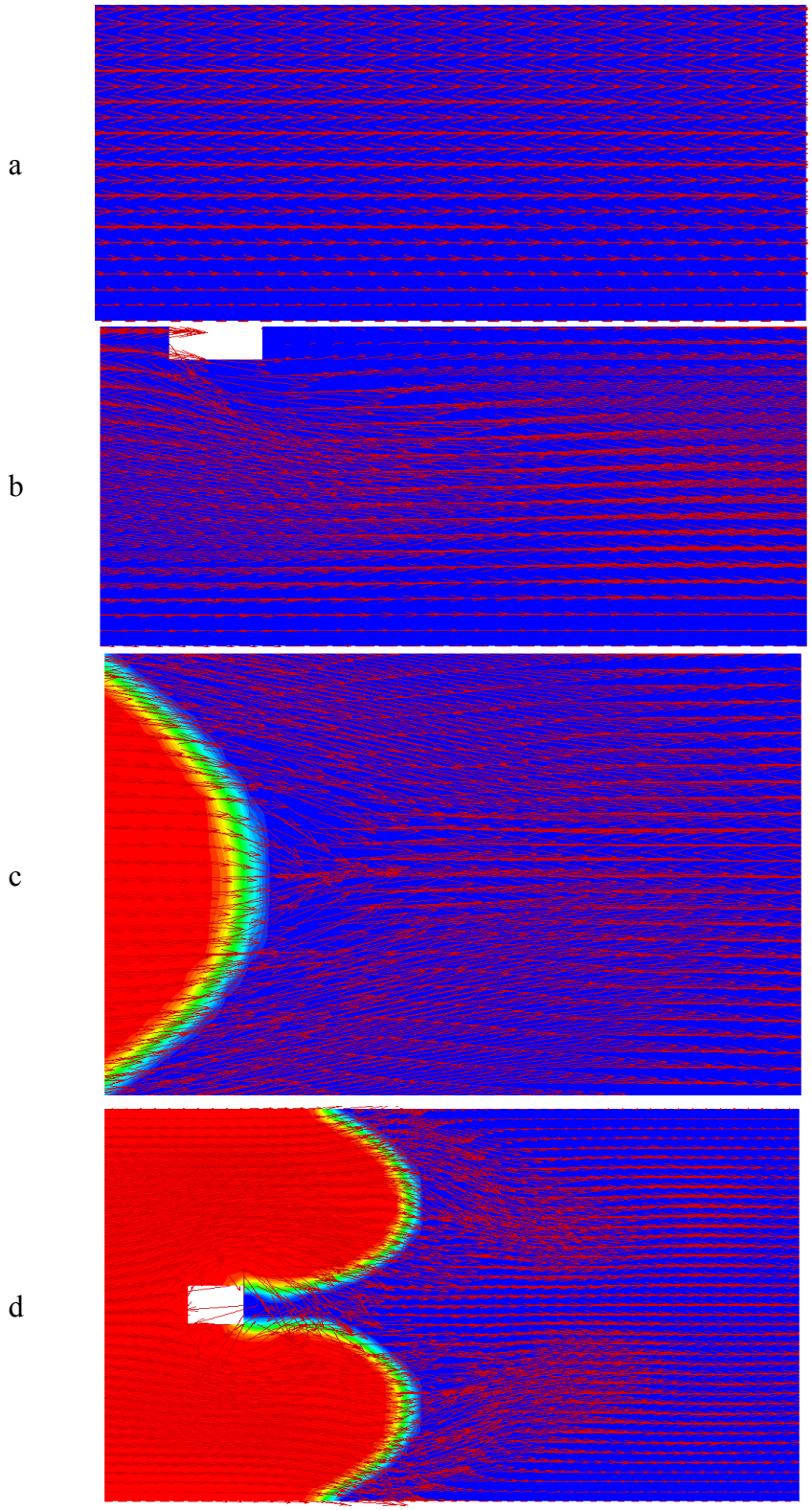

Figure 4.7: Velocity vector for (a) Water Flow (b) Water Flow around an obstacle (c) Leading edge of Taylor bubble (d) Leading edge of Taylor bubble as it flow past the obstacle at the center of the channel.

Figure 4.7(a-b) shows only half width of the microchannel (wall at the lower edge) while Figure 4.7(c-d) shows full width of the microchannel. In Fig. 4.7(a) it can be observed that the velocity vectors are parallel to each other and their magnitude are smaller towards the wall (lower edge) and bigger towards the center, as per the conventional theory of fluid flow through a surface. Due to laminar flow nature there will be no mixing of fluid in the channel. Figure 4.7(b) represents liquid flow past the square obstacle, where some amount of turbulence in velocity vector can be observed. This is due to disturbance created by presence of obstacle and due to wake in this region, which is a very well-studied phenomenon.

Figure 4.7(c) shows the velocity vector in front of advancing meniscus of the Taylor bubble. Here some amount of mixing can be observed in the liquid region in front of the gas bubble. This is due to mixing and recirculation characteristics of gas-liquid Taylor bubble flow as reported in many existing studies [25-28]. Figure 4.7(d) shows velocity vectors as the advancing meniscus of the Taylor bubble flows past the square obstacle positioned at the channel center. As described earlier in Fig. 4.1(e), now two smaller meniscuses emerge from both sides of the obstacle and later merge to form the original meniscus. Because of the continuous change in the shape of the advancing meniscus i.e. the liquid-gas interface, the liquid particles ahead of this meniscus also additionally move continuously in a direction perpendicular to the flow direction. This causes more turbulence because of combined effects shown in Fig. 4.7(b-c). Thus, the mixing and turbulence are highest when a Taylor bubble flows past an obstacle as compared to only Taylor bubble flow or liquid flow past an obstacle. This can be observed from both the magnitude and direction of the velocity vectors shown in

Fig. 4.7(d). Thus, this concept can be used to enhance heat and mass transfer in microchannel systems where achieving turbulence and mixing is comparatively difficult though many engineering applications demand the same.

Chapter –5

Conclusion

A two-dimensional numerical study has been carried out to understand the effect of an obstacle, at different positions along the cross section, on the Taylor bubble flow in micro channel. The flow is laminar, water velocity and gas velocity at inlet is 0.251m/s and 0.0073m/s respectively. The microchannel diameter is 0.2 mm and a square obstacle of side 0.02 mm is used inside the microchannel. Air and water enters the channel from two different inlets. Both inlets are placed perpendicular to each other. Thus, the Taylor bubble is created at the T-joint and flows downward along the channel.

The obstacle is placed at a distance sufficiently away from the T-junction to ensure stability of the Taylor bubble by the time it touches the obstacle. The position of the obstacle is varied by moving it along the perpendicular to the fluid flow direction by considering its center's distance y from the right wall. First the obstacle is placed exactly at the center of the channel such that y = 0.1. In such case there will be equal space of 0.09 mm each on the both sides of the obstacle through which the fluid can flow. As the Taylor bubble touches the obstacle the tip of the front meniscus splits in to two, and moves through both sides of the obstacle with perfect symmetric flow. The bubbles rejoin to form the original bubble as it moves past the obstacle. Next, the obstacle is moved by 0.02 mm away from the center line towards the right, thus providing a gap of 0.11 mm and 0.07 mm on the left and the right sides of the obstacle respectively. Now it is found that as the bubble touches the obstacle it moves through the bigger opening of 0.11 mm only and water flows through the smaller opening of 0.07 mm only. Unlike previous case, in this case no split in the bubble is observed. Similar phenomena are observed when the obstacle is further moved away from the center line towards one side. The water-air interface is found to be continuously changing its shape due to disturbance created by the presence of an obstacle. This creates turbulence inside the liquid plug. This increases anticipation to enhance heat and mass transfer in microchannel systems by placing multiple obstacles.

References:

1. Angeli, P., and Gavriilidis, A., 2008, “Taylor flow in microchannels,” In: Li, D., (ed.) Encyclopedia of Microfluidics and Nanofluidics. (1971 - 1976). Springer: New York.
2. Garstecki, P., Fuerstman, M. J., Stone, H. A., and Whitesides, G. M., 2006, “Formation of droplets and bubbles in a microfluidic T – junction - scaling and mechanism of break-up,” Lab on a Chip, 6, pp. 437-446.
3. Yue, J., Luo, L., Gonthier, Y., Chen, G., and Yuan, Q., 2008, “An experimental investigation of gas-liquid two-phase flow in single microchannel contactors,” Chemical Engg. Science, 63(16), pp. 4189-4202.
4. Salman, W., Gavriilidis, A., and Angeli, P., 2006, “On the formation of Taylor bubbles in small tubes,” Chemical Engg. Science, 61, pp. 6653-6666.
5. Gibson, A. H., 1913, “On the motion of long air-bubbles in a vertical tube,” Philosophical Magazine Series 6, 26(156), pp. 952-965.
6. Fairbrother, F., and Stubbs, A. E., 1935, “Studies in electro-endosmosis. Part VI. The “bubble-tube” method of measurement,” J. Chem. Soc., 1, pp. 527–529.
7. Taylor, G. I., 1961, “Deposition of a viscous fluid on the wall of a tube,” J. Fluid Mech., 10, pp. 161-165.
8. Triplett, K.A., Ghiaasiaan, S.M., Abdel- Khalik, S.I., and Sadowski, D.L., Gas–liquid two-phase flow in micro channels, Int. J. Multiphase Flow, vol. 25, no. 3, pp. 377–394, 1999.
9. Kishimoto, T., and Sasaki S., 1987, “Cooling characteristics of diamond-shaped interrupted cooling fin for high-power LSI devices,” Electronic Letters, 23(9), pp. 456-457.
10. Zhao, T.S. and Bi, Q.C.,”Co-current air–water two phase flow patterns in vertical triangular micro channels”, Int. J. Multiphase Flow, vol. 27, no. 5, pp.765–782, 2001.
11. Liu H., Vandu C.O., Krishna R., 2005. Hydrodynamics of Taylor flow in vertical capillaries: Flow regimes, bubble rise velocity, liquid slug length, and pressure drop. Industrial & Engineering Chemistry Research 44, 4884–4897.
12. Qian, D., and Lawal, A., 2006, “Numerical study on gas and liquid slugs for Taylor flow in a T-junction micro channel,” Chemical Engg. Science 61, pp. 7609-7625.
13. Baroud C. N., Gallaire F., and Dangla R., “Dynamics of microfluidic droplets,” Lab on a Chip, vol. 10, no. 16, pp. 2032– 2045, 2010.

14. Santos, R. M., and Kawaji, M., 2010, “Numerical modeling and experimental investigation of gas-liquid slug formation in a microchannel T-junction,” Int. J. Multiphase Flow, 36(4), pp. 314-323.
15. Yang Z.C., Bi Q.C., Liu B., Huang K.X., 2010. Nitrogen/non-Newtonian fluid two-phase upward flow in non-circular micro channels. International journal of multiphase flow 36, 60-70.
16. Zhang T, Cao B., Fan Y., Gonthier Y., Luo L., Wang S., 2011. Gas liquid flow in circular micro channel. Part.1- Influence of liquid physical properties and channel diameter on flow patterns. Chemical engineering science 66, 5791-5803.
17. Pham, H., Wen, L., and Zhang, H., 2012 “Numerical simulation and analysis of gas-liquid flow in a T-junction microchannel,” Adv. Mech. Engg., pp. 1-8.
18. Rubio-Jimenez, C. A., Kandlikar, S. G., and Hernandez-Guerrero, A., 2012, “Numerical analysis of novel micro pin fin heat sink with variable fin density,” IEEE Trans. Components, Packaging Mfg. Tech., 2(5), pp. 825-833.
19. Thulasidas, T. C., Abraham, M. A., and Cerro, R. L., 1997, “Flow patterns in liquid slugs during bubble-train flow inside capillaries,” Chemical Engg. Science, 52(17), pp. 2947-2962.
20. Krepper, E., Lucas, D., Frank, T., Prasser, H.M., Zwart, P. J., 2008. The inhomogeneous MUSIG model for the simulation of polydispersed flows. Nucl. Eng. Des. 238(7), pp. 1690–1702.
21. Majumder, A., Mehta, B., and Khandekar, S., 2013, “Local Nusselt number enhancement during gas-liquid Taylor bubble flow in a square mini-channel: An experimental study,” Int. J. Thermal Science, 66, pp. 8-18.
22. Gupta, R., Fletcher, D. F., and Haynes, B. S., 2009, “On the CFD modelling of Taylor flow in microchannels,” Chemical Engg. Science, 64(12), pp. 2941-2950.
23. Bretherton, F. P., 1961, “The motion of long bubbles in tubes,” J. Fluid Mechanics, 10(2), pp 166-188.
24. Zaloha, P., Kristal, J., Jiricny, V., Völkel, N., Xuereb, C., and Aubin, J., 2012, “Characteristics of liquid slugs in gas–liquid Taylor flow in microchannels,” Chemical Engg. Science, 68(1), pp. 640-649.
25. Abadie, T., Xuereb, C., Legendre, D., and Aubin, J., 2013, “Mixing and recirculation characteristics of gas–liquid Taylor flow in microreactors,” Chemical Engg. Research Design, 91(11), pp. 2225-2234.

26. Abiev, R. S., 2013, “Bubbles velocity, Taylor circulation rate and mass transfer model for slug flow in milli- and microchannels,” Chemical Engg. J., 227, pp. 66-79.
27. Mehta, B., Khandekar, S., 2014, “Measurement of local heat transfer coefficient during gas–liquid Taylor bubble train flow by infra-red thermography,” Int. J. Heat Fluid Flow, 45, pp. 41-52.
28. Hibiki T., Mishima K., 2001. Flow regime transition criteria for upward two-phase flow in vertical narrow rectangular channel. Nucl Eng. Des. 203, 117–131.
29. Prasser, H.-M., Krepper, E., Lucas, D., 2002. Evolution of the two-phase flow in a vertical tube—decomposition of gas fraction profiles according to bubble size classes using wire-mesh sensors. Int. J. Thermal Sci. 41, 17–28.
30. Zwart, P., Burns, A.,Montavon, C., 2003. Multiple size group models. Technical Report. AEA Technology plc., November, 2003. CFX-5.7.
31. Waelchli S., Rudolf von Rohr., 2006. Two-phase flow characteristics in gas–liquid micro reactors. International Journal of Multiphase Flow 32, 791–806.
32. Lucas, D., Krepper, E., Prasser, H.-M., 2007. Use of models for lift, wall and turbulent dispersion forces acting on bubbles for poly-disperse flows. Chem. Sci. Eng. 62, 4146–4157.
33. Khandekar, S., Panigrahi, P.K., Lefevre, F., and Bonjour, J., Local hydrodynamics of flow in a pulsating heat pipe: A review, Front. Heat Pipes, vol. 1, p. 023003, 2010.